Acta Crystallographica Section F
Structural Biology and Crystallization Communications
ISSN 1744-3091

Structure of anti-FLAG M2 Fab domain and its use in the stabilization of engineered membrane proteins

Tarmo P. Roosild,‡ Samantha Castronovo‡ and Senyon Choe*

Structural Biology Laboratory, The Salk Institute for Biological Studies, La Jolla, California 92037, USA

‡ Current address: Drug Development Division, Nevada Cancer Institute, Las Vegas, Nevada 89135, USA.

Correspondence e-mail: choe@salk.edu

Received 28 March 2006
Accepted 27 July 2006

PDB Reference: anti-FLAG M2 Fab domain, 2g60, r2g60sf.

The inherent difficulties of stabilizing detergent-solubilized integral membrane proteins for biophysical or structural analysis demand the development of new methodologies to improve success rates. One proven strategy is the use of antibody fragments to increase the 'soluble' portion of any membrane protein, but this approach is limited by the difficulties and expense associated with producing monoclonal antibodies to an appropriate exposed epitope on the target protein. Here, the stabilization of a detergent-solubilized K^+ channel protein, KvPae, by engineering a FLAG-binding epitope into a known loop region of the protein and creating a complex with Fab fragments from commercially available anti-FLAG M2 monoclonal antibodies is reported. Although well diffracting crystals of the complex have not yet been obtained, during the course of crystallization trials the structure of the anti-FLAG M2 Fab domain was solved to 1.86 Å resolution. This structure, which should aid future structure-determination efforts using this approach by facilitating molecular-replacement phasing, reveals that the binding pocket appears to be specific only for the first four amino acids of the traditional FLAG epitope, namely DYKD. Thus, the use of antibody fragments for improving the stability of target proteins can be rapidly applied to the study of membrane-protein structure by placing the short DKYD motif within a predicted peripheral loop of that protein and utilizing commercially available anti-FLAG M2 antibody fragments.

1. Introduction

Integral membrane (IM) proteins constitute nearly a third of the proteins of sequenced genomes and comprise more than half of the targets of blockbuster drugs. However, these important proteins remain largely structurally and biophysically uncharacterized, partly as a consequence of the daunting difficulties their amphipathic chemistry presents for analysis by traditional methods. In order to retain these proteins in homogeneous populations of native conformation, detergents must be employed to substitute for the cell membrane's lipid bilayer. Detergents, however, tend to destabilize the fold of the protein and also mask the protein's surface. Only a few alternatives to the use of detergent have been put forward (Schafmeister *et al.*, 1993; Ostermeier & Michel, 1997; McGregor *et al.*, 2003). Some effort has been made recently to reengineer IM proteins, including their transmembrane domains, into soluble homologues that do not require detergents to prevent aggregation, either by mutagenesis (Li *et al.*, 2001; Slovic *et al.*, 2003, 2004; Roosild & Choe, 2005) or covalent modification (Becker *et al.*, 2004). However, these endeavors have not yet yielded structural data nor has it been demonstrated whether such drastic modification can be accomplished without distorting the intrinsic structure of the IM protein in question. Semi-polar organic solvents able to accommodate both the hydrophobic and hydrophilic portions of an IM protein have been suggested as another alternative, but to date such studies have rarely been productive (Garavito *et al.*, 1996). The use of bicelles (Faham & Bowie, 2002; Faham *et al.*, 2005) or cubic lipid phases (Landau & Rosenbusch, 1996) appears promising for better stabilizing IM proteins in their native conformations, but neither addresses the lack of solvent-exposed residues needed for the application of many structural and biophysical techniques.

One tool structural biologists have employed in cases of difficult to analyze proteins is the use of monoclonal antibody fragments (Kovari *et al.*, 1995). The binding of Fab domains to a target protein ligand can improve its stability and solubility and even provide a scaffold for protein crystallization (Stura *et al.*, 2002). Fab bound to the target IM protein increases the relative proportion of hydrophilic surface area available for crystal contact formation and thus improves the chances of successful crystallization (Hunte & Michel, 2002; Rothlisberger *et al.*, 2004). This technique has proven its value with cytochrome *c* oxidase (Ostermeier *et al.*, 1995), cytochrome bc_1 complex (Hunte *et al.*, 2000) and, more recently, the potassium channels KcsA (Zhou *et al.*, 2001) and KvAP (Jiang *et al.*, 2003) and the chloride channel ClC (Dutzler *et al.*, 2003). Many of these structures could not have been determined or would have been analyzed at significantly lower resolution but for the utilization of antibody fragment-mediated crystallization. However, the expense and difficulty of raising the necessary monoclonal antibodies and producing them in sufficient quantity from hybridomas using conventional protocols has severely restricted the utility of this protocol and necessitated the development of alternative techniques (Shea *et al.*, 2005). Another inherent weakness of the traditional process is that one must arduously screen for an antibody that can bind specifically to an exposed, preferably peripheral, loop of the target IM protein in order to cause minimal structural distortion. One possible solution to overcome these obstacles is to use monoclonal antibodies with known peptide-binding epitopes (Kaufmann *et al.*, 2002). This can allow systematic engineered introduction of the required motif at optimal locations within the target IM protein, chosen based on available knowledge concerning the IM protein under investigation, so as to minimize the potential for deformation of the structure. Here, we report the structure of anti-FLAG M2 Fab (Fab M2), a potentially useful model for molecular-replacement phasing of future structures solved in complex with this domain, and describe its epitope-binding pocket. The potential of this approach to stabilize IM proteins is also demonstrated using a potassium channel, KvPae, with an engineered FLAG epitope as a test case.

2. Methods

2.1. Protein preparation

Anti-Flag M2 antibody was obtained from Sigma and processed to Fab fragments by immobilized ficin digestion followed by filtration on an immobilized Protein A column using a commercially available kit (Pierce). Fab M2 fragments were purified further by FPLC gel filtration on a Superdex S-75 column (Pharmacia). Cleavage and purification yielded ~2 mg of Fab from 5 mg starting antibody. KvPae (GenBank ID 15596693) from *Pseudomonas aeruginosa* was cloned into an octahistidine-tagged variant of pET15 (Novagen) for N-terminally His-tagged expression with an intervening Mistic fusion domain (Roosild *et al.*, 2005). The FLAG epitope (DYKDDDDK) with flanking glycines was added in place of Gly54 of KvPae by whole plasmid PCR with *Pfu* polymerase (Stratagene), followed by *Spe*I and *Dpn*I digestion for 1 h at 310 K and T4 ligation of purified products (all enzymes from NEB). Oligo sequences were forward primer, CTAGACTAGTACGATAAGGGCCAGGACTACGGCC-GACTG; reverse primer, GATCACTAGTCTTTGTAGTCGCCCC-TGGTGGATTTCGTCGATG. *Escherichia coli* BL21 (DE3) cells were transformed with the modified plasmid, grown at 310 K to an optical density of 1.0 at 600 nm, induced with 0.1 m*M* IPTG and then incubated for 16 h at 288 K. Cells were harvested by centrifugation (5000*g*), resuspended in buffer *A* (50 m*M* Tris pH 8.0, 300 m*M* KCl, 10 m*M* imidazole, 10 m*M* β-ME) with 1 mg ml^{-1} lysozyme and lysed by sonication on ice. Mistic fused KvPae was solubilized from bacterial membranes collected after high-speed centrifugation (100 000*g*) by resuspension in buffer *A* with 10 m*M* LDAO and purified by Ni–NTA affinity chromatography (Novagen). KvPae was separated from both Mistic and the His tag by overnight digestion with thrombin at 277 K. Complexes between KvPae and Fab M2 were formed by overnight incubation of equimolar amounts of the two proteins at 277 K. The protein concentrations of KvPae and Fab M2 were initially determined by theoretical extinction coefficients that were further calibrated based on the detection of excess unbound Fab fragment during subsequent analysis. Resulting complexes were analyzed by either native PAGE or gel filtration on a Superose-6 column (Pharmacia) with 5 m*M* LDAO retained in the running buffer (20 m*M* Tris pH 8.0, 150 m*M* KCl).

Table 1
Summary of crystallographic data and model refinement statistics.

Source	ALS
Wavelength (Å)	1.00
Space group	$P2_12_12$
Unit-cell parameters (Å)	a = 87.36, b = 133.76, c = 41.48
Mosacity (°)	0.37
Resolution (Å)	50–1.86 (1.94–1.86)
R_{sym} (%)	3.3 (19.4)
$I/\sigma(I)$	34.4 (3.9)
Completeness (%)	92.3 (75.2)
Resolution (Å)	50–1.86
No. of reflections	40450
No. of monomers in ASU	1
Atoms in ASU	
Protein	3250
Water	384
R_{cryst} (%)	23.5
R_{free} (%)	27.8
R.m.s.d. bond lengths (Å)	0.020
R.m.s.d. bond angles (°)	2.07
Ramachandran statistics (%)	
Favored regions	87.3
Allowed regions	11.6

2.2. Crystallization, data collection and data processing

Using the purified complex of KvPae–Fab M2 (5 mg ml^{-1}) as the starting material, crystal screening using the sparse-matrix approach (Hampton) was conducted using hanging-drop vapor-diffusion methods (2 µl protein:2 µl reservoir) at room temperature and at 277 K (~1000 trials in total). Crystals of Fab M2 grew at room temperature by the hanging-drop vapor-diffusion method against reservoirs containing 15% PEG 4000 with 100 m*M* ammonium sulfate. These conditions produced crystals of the Fab M2 fragment alone that grew to 200 µm in size over 1–2 weeks. Crystals were stabilized briefly in cryoprotectant containing 25% glycerol in addition to the contents of the reservoir prior to freezing by rapid immersion in liquid nitrogen. Data sets were collected at the Advanced Light Source (ALS) synchrotron, beamline 8-3 (Table 1). Image processing and data integration were accomplished with *HKL*-2000 (Otwinowski & Minor, 1997) in addition to the *CCP*4 suite of programs (Collaborative Computational Project, Number 4, 1994). A molecular-replacement solution was found with *MOLREP* (Vagin & Teplyakov, 1997) using the structure of monoclonal 6B5 Fab (Lim *et al.*, 1998; PDB code 2pcp) as a search model following separation of the two flexibly linked individual immunoglobulin folds. The strongest signal was found using initially only the variable domain, resulting in a rotation-function solution with Rf/σ = 9.00 (next highest Rf/σ = 6.57, corresponding to the placement of the variable domain of

the model in the orientation of the constant domain in the crystal; remaining solutions had Rf/σ < 4.33). A translation search produced a unique solution with Tf/σ = 11.74 (next best solution 8.23), correlation coefficient = 0.293 (0.216) and *R* factor = 0.533 (0.565). Rounds of model building in *O* (Jones & Kjeldgaard, 1997) and refinement in *CNS* (Brünger *et al.*, 1998) resulted in the final structure. *PROCHECK* (Laskowski *et al.*, 1993) analysis was used for structure validation. Figures were generated using *MOLSCRIPT* (Kraulis, 1991) and rendered with *POV-Ray* (http://www.povray.org). Surfaces and electrostatic potentials were depicted using *MOLMOL* (Koradi *et al.*, 1996).

3. Results and discussion

To explore the potential of commercially available anti-FLAG monoclonal antibodies as tools in membrane-protein structural biology, a test protein was chosen: a bacterial voltage-gated K^+ channel homolog from *P. aeruginosa*, KvPae. This protein consists of six transmembrane segments (S1–S6) that assemble as homotetramers. Notably, the protein has virtually no extracellularly exposed domains, severely limiting the available surface on this face of the channel for biochemical analysis or crystal lattice formation. Additionally, like many IM proteins, detergent-solubilized KvPae is prone to time- and concentration-dependent aggregation, further lessening its suitability for study by most techniques. Into the middle of the first intra-transmembrane helix loop, between S1 and S2, the FLAG epitope was added, bracketed by glycines to provide limited orientation flexibility to promote binding of the antibody (Fig. 1*a*). The detergent-solubilized behavior of KvPae bound to the Fab M2 fragment was assessed by size-exclusion chromatography and the complex between anti-FLAG M2 Fab and modified KvPae was found to be monodisperse without any indication of higher order aggregation (Fig. 1*b*), in stark contrast to KvPae by itself. The complex between KvPae and Fab M2 can be concentrated to >5 mg ml^{-1} and remains soluble for weeks at 277 K without any indication of denaturation or precipitation, whereas unbound KvPae shows visible signs of aggregation within 24 h at similar or even lower protein concentrations.

In the process of screening possible crystallization conditions for this complex, well ordered crystals of Fab M2 in isolation were grown that diffracted X-rays beyond 1.8 Å. Presumably, the chemical environment of this particular condition led to dissociation of the complex followed by crystallization of only the antibody domain. In order to better understand how to optimize the use of Fab M2 in this approach, its structure determination was undertaken. Whereas molecular-replacement phasing of the diffraction data was accomplished in a straightforward manner using other Fab structures as search models, structure refinement could not proceed further owing to the lack of Fab M2 primary sequence, as *a priori* knowledge of Fab M2 was limited to the antibody class (mIgG1), which provides only ~75% of the sequence based on strict residue conservation. This limitation was eventually overcome by N-terminal degradation sequencing of the first 40 residues of the light chain. Based on this data, the closest homolog in the PDB (PDB code 2pcp) was identified and was used along with its associated heavy chain as a starting model for structure refinement (Fig. 2*a*). Next, annealed composite OMIT maps were used to identify residues that did not fit the electron-density maps. In these cases, lacking the primary sequence of the protein, the residue was modeled as an alanine to produce an initial experimental structure for Fab M2. In all, there are seven light-chain residues and 31 heavy-chain residues that were truncated to alanine (marked '?' in Fig. 2*a*). Subsequently, a second model was built mutating these residues to the amino acid that best fitted the electron-density map or, if an unambiguous assignment of residue type could not be assessed from the maps, to the most closely fitting residue from a limited list of choices derived from the ten closest Fab homologues to the starting model in GenBank. This process yielded a

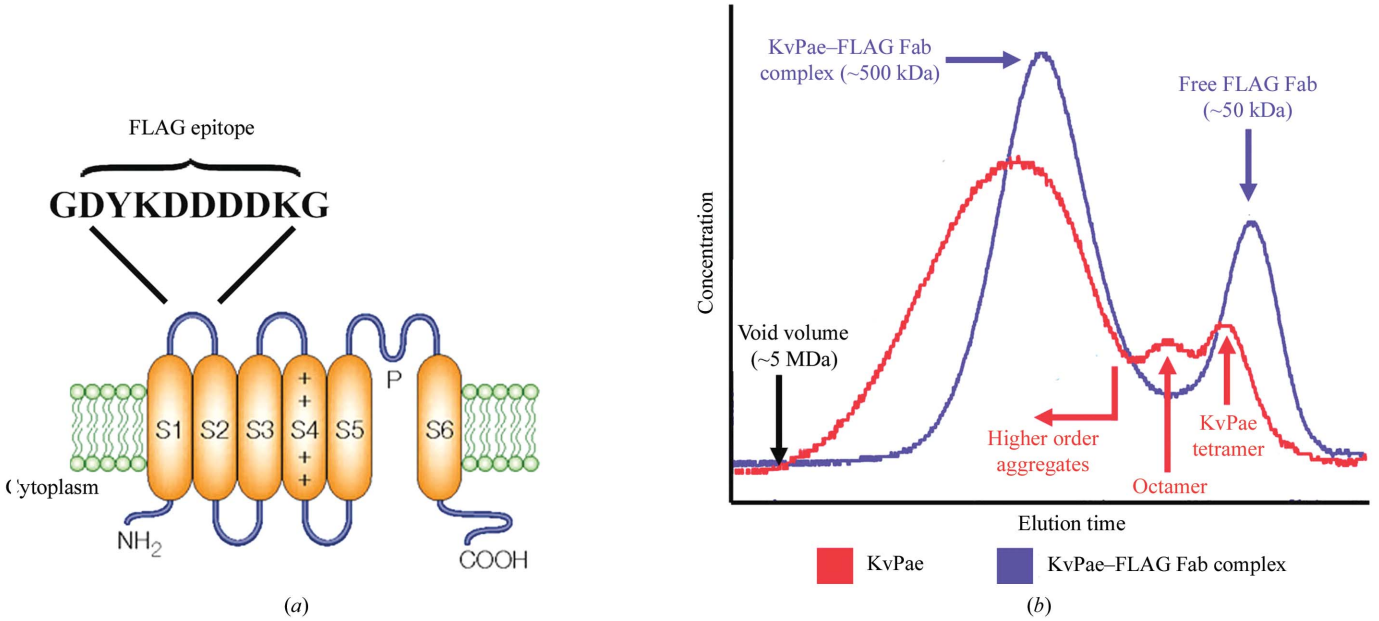

Figure 1
Anti-FLAG antibody binding to the K^+ channel KvPae promotes its detergent-solubilized stability. (*a*) Topology of KvPae with six transmembrane segments (S1–S6) and a re-entrant loop forming the K^+ ion-selectivity filter (P) showing the location of the inserted FLAG epitope. The ten amino acids shown replaced a single glycine (residue 54) in the native protein. (*b*) Gel-filtration analysis of LDAO-solubilized KvPae (32 kDa) reveals a spectrum of oligomers ranging in size from tetrameric to aggregates up to the 5 MDa void volume of the column (red). In contrast, the KvPae–Fab M2 complex elutes as a symmetrical monodisperse peak of the expected size [(32 kDa KvPae + 50 kDa Fab) × 4 (*i.e.* homotetramer) + ~150 kDa detergent micelle = 478 kDa] (blue).

theoretical model for Fab M2 and improved R_{cryst} and R_{free} from 32.5 to 28.2% and from 36.4 to 31.5%, respectively. The final refined R_{cryst} and R_{free} for the theoretical model are 23.5 and 27.8%, respectively. While these R factors are slightly higher than expected given the resolution of the data, this can partly be attributed to an anomaly of the crystal, namely that the constant domain of the Fab fragment is significantly less ordered than the variable domain (Fv), as reflected by the substantially higher refined B factors in this half of the structure (Fig. 2*b*).

Analysis of the final theoretical model reveals that the most prominent feature of the antigen-binding surface, which is distant from any distorting crystal contact interfaces, is a deep highly negatively charged pit (Fig. 3*a*). At the base of this cavity, a single glutamate residue appears to be a likely candidate to form a salt

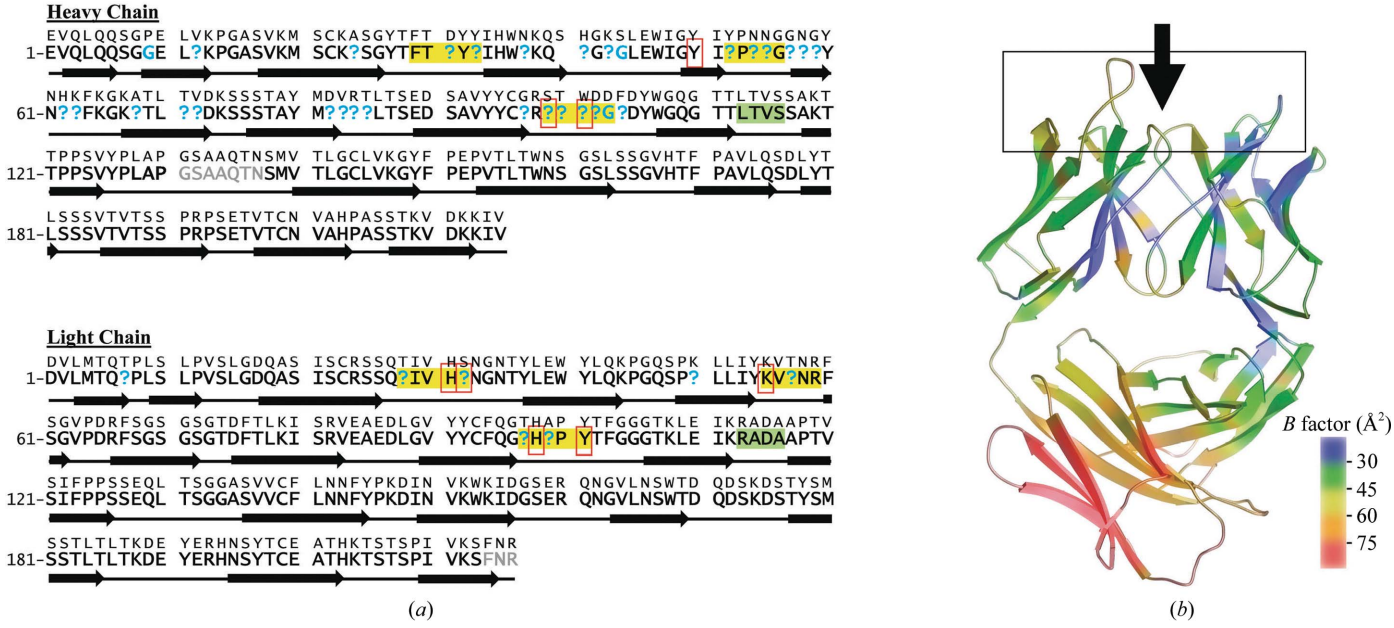

Figure 2
Anti-FLAG M2 Fab primary sequence and structure. (*a*) The experimentally deduced primary sequence of the Fab M2 domains and secondary-structure boundaries are shown (large letters). Residues in black are conserved in the most homologous Fab (by comparison of light chains) of known structure (monoclonal 6B5 Fab; PDB code 2pcp; small letters). Residues that did not match the electron-density maps are indicated with '?' in blue and were modeled as alanine in the experimental structure. The hypervariable loops are highlighted in yellow and the loops connecting the adjoining Ig folds are marked in green. Red boxes indicate residues that are likely to be involved in epitope binding based on positioning and side-chain orientation. Residues omitted from the refined structure owing to lack of electron density in maps are indicated in grey. (*b*) Ribbon illustration showing the Fab M2 structure colored by B factor, with the variable domain (Fv) toward the top. The higher B factors in the lower constant domain are probably indicative of more global disorder in this region of the crystal lattice. The hypervariable loops are boxed and the viewpoint of Fig. 3 into the epitope-binding site formed by the three hypervariable loops from both the heavy and light chains is indicated by an arrow.

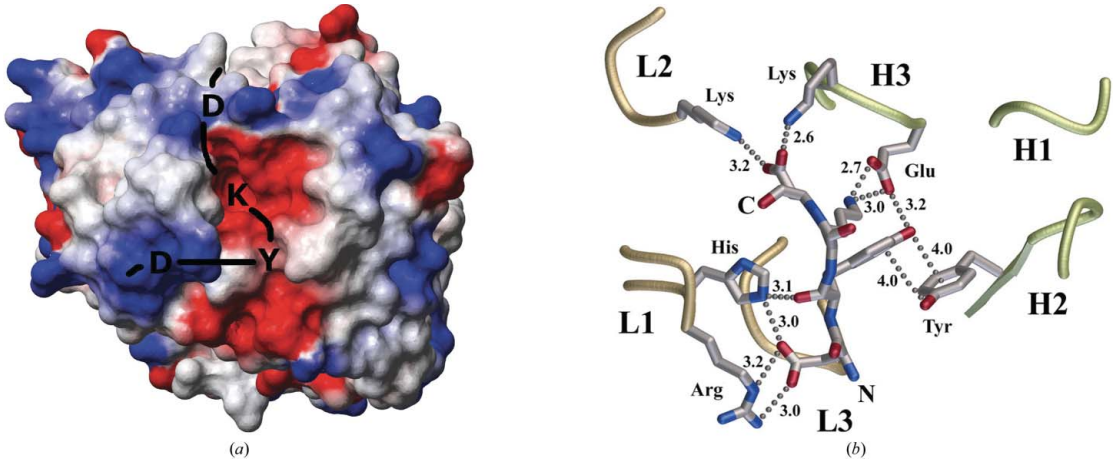

Figure 3
Characteristics of the anti-FLAG M2-binding pocket. (*a*) Surface rendering of the binding surface of the theoretical model of the anti-FLAG M2 antibody (boxed in Fig. 2, from the viewpoint of the arrow) is shown colored by electrostatic potential (red, negative; blue, positive). The most significant features of the binding pocket are a deep highly acidic pit (center) and two highly basic ridges above and to the left of this hollow. The illustrated chemistry strongly suggests a binding orientation for the first four residues of the FLAG motif (DYKD) and the exclusion of the remainder of the motif from direct specific interaction within the binding pocket of the antibody. (*b*) Diagram showing the positioning of hypervariable loops (L1–3, H1–3) and critical residues of the theoretical model from the same orientation and on the same scale as (*a*). One possible model for the binding conformation of the shortened FLAG epitope is illustrated, fitted with reasonable geometry and chemistry. Numbers indicate the interatomic distances of heavy atoms in Å.

bridge with the lysine of the FLAG epitope. Adjoining the acidic hollow are two conserved tyrosine residues, either or both of which may be capable of π-bond formation with the sole tyrosine of the FLAG epitope. Surrounding these two elements are two clusters of positively charged residues, each presumably capable of coordinating a single aspartate of the highly negatively charged FLAG motif. A modeled tetrapeptide can be fitted with reasonable shape, geometry and compatible chemistry (Fig. 3*b*). It is unlikely, given the geometrical positioning of the aforementioned features and the relative size and location of the hypervariable loops of the antibody, that significant binding specificity exist beyond these four residues. This is consistent with an earlier report that the anti-FLAG M1 antibody has no loss in affinity when the larger FLAG epitope was reduced to DYKD (Knappik & Plückthun, 1994) and a phage-display study that also affirmed a four-residue binding interface (Miceli *et al.*, 1994).

The extraneous four residues (DDDK) of the conventional FLAG motif may improve accessibility of the binding epitope in some applications by adding flexibility to the peptide or by displacing it from the linked protein, while simultaneously providing an enterokinase cleavage site. However, for the purposes of using Fab M2 for structural biophysics, where excessive interdomain flexibility may be detrimental to certain methods such as crystallization, it is worth noting that DYKD is a sufficient epitope for binding Fab M2. Additionally, this reduces the number of residues to be introduced into a target protein by half, reducing the likelihood of adverse conformational deformation by the engineered modification. We have demonstrated here that beyond the initial intended purpose of encircling an IM protein with Fab antibody fragments in order to enlarge the hydrophilic surface area available for crystal contact formation, Fab binding can also beneficially deter adverse aggregation of detergent-solubilized IM proteins. This is likely to be achieved by sterically prohibiting micelle amalgamation.

As we have shown, the shortened FLAG motif can be rapidly introduced to peripheral extramembraneous loops in a target protein, alleviating the current prerequisite to antibody-mediated stabilization of IM proteins that the desirable binding location must be antigenic. When utilized in combination with affordable commercially available anti-FLAG monoclonal antibodies, this can be a valuable tool for the biophysical or structural analysis of such proteins. Furthermore, the ability to introduce the short binding epitope systematically at variable locations within the target protein, guided by its membrane topology, allows the selection of complexes without undesirable conformational changes induced by antibody binding. Naturally, the availability of the Fab M2 structure reported here will expedite subsequent structure determination of any crystallized complexes by augmenting molecular-replacement phasing methods.

The authors thank C. Park for Edman degradation sequencing of proteins. This work was conducted in part at the Advanced Light Source (ALS), which is funded by the Department of Energy, Office of Biological and Environmental Research. We thank the staff of crystallographic beamlines at ALS for assistance with data collection. This work was supported by the NIH (GM6653, GM74821).

References

Becker, C. F. W., Strop, P., Bass, R. B., Hansen, K. C., Locher, K. P., Ren, G., Yaeger, M., Rees, D. C. & Kochendoerfer, G. G. (2004). *J. Mol. Biol.* **343**, 747–758.
Brünger, A. T., Adams, P. D., Clore, G. M., DeLano, W. L., Gros, P., Grosse-Kunstleve, R. W., Jiang, J.-S., Kuszewski, J., Nilges, M., Pannu, N. S., Read, R. J., Rice, L. M., Simonson, T. & Warren, G. L. (1998). *Acta Cryst.* D**54**, 905–921.
Collaborative Computational Project, Number 4 (1994). *Acta Cryst.* D**50**, 760–763.
Dutzler, R., Campbell, E. B. & MacKinnon, R. (2003). *Science*, **300**, 108–112.
Faham, S., Boulting, G. L., Massey, E. A., Yohannan, S., Yang, D. & Bowie, J. U. (2005). *Protein Sci.* **14**, 836–840.
Faham, S. & Bowie, J. U. (2002). *J. Mol. Biol.* **316**, 1–6.
Garavito, R. M., Picot, D. & Loll, P. J. (1996). *J. Bioenerg. Biomembr.* **28**, 13–27.
Hunte, C., Koepke, J., Lange, C., Rossmanith, T. & Michel, H. (2000). *Structure*, **8**, 669–684.
Hunte, C. & Michel, H. (2002). *Curr. Opin. Struct. Biol.* **12**, 503–508.
Jiang, Y., Lee, A., Chen, J., Ruta, V., Cadene, M., Chait, B. T. & MacKinnon, R. (2003). *Nature (London)*, **423**, 33–41.
Jones, T. A. & Kjeldgaard, M. O. (1997). *Methods Enzymol.* **277**, 173–208.
Kaufmann, M., Lindner, P., Honegger, A., Blank, K., Tschopp, M., Capitani, G., Plüchthun, A. & Grutter, M. G. (2002). *J. Mol. Biol.* **318**, 135–147.
Knappik, A. & Plückthun, A. (1994). *Biotechniques*, **17**, 754–761.
Koradi, R., Billeter, M. & Wuthrich, K. (1996). *J. Mol. Graph.* **14**, 29–32.
Kovari, L. C., Momany, C. & Rossmann, M. G. (1995). *Structure*, **3**, 1291–1293.
Kraulis, P. J. (1991). *J. Appl. Cryst.* **24**, 946–950.
Landau, E. M. & Rosenbusch, J. P. (1996). *Proc. Natl Acad. Sci. USA*, **93**, 14532–14535.
Laskowski, R. A., MacArthur, M. W. & Thornton, J. M. (1993). *J. Appl. Cryst.* **26**, 283–291.
Li, H., Cocco, M. J., Steitz, T. A. & Engelman, D. E. (2001). *Biochemistry*, **40**, 6636–6645.
Lim, K., Owens, S. M., Arnold, L., Sacchettini, J. C. & Linthicum, D. S. (1998). *J. Biol. Chem.* **273**, 28576–28582.
McGregor, C. L., Chen, L., Pomroy, N. C., Hwang, P., Go, S., Chakrabartty, A. & Privé, G. G. (2003). *Nature Biotechnol.*, **21**, 171–176.
Miceli, R. M., DeGraaf, M. E. & Fischer, H. D. (1994). *J. Immunol. Methods*, **167**, 279–287.
Ostermeier, C., Iwata, S., Ludwig, S. & Michel, H. (1995). *Nature Struct. Biol.* **2**, 842–846.
Ostermeier, C. & Michel, H. (1997). *Curr. Opin. Struct. Biol.* **7**, 697–701.
Otwinowski, Z. & Minor, W. (1997). *Methods Enzymol.* **276**, 307–326.
Roosild, T. P. & Choe, S. (2005). *Protein Eng. Des. Sel.* **18**, 79–84.
Roosild, T. P., Greenwald, J., Vega, M., Castronovo, S., Riek, R. & Choe, S. (2005). *Science*, **307**, 1317–1321.
Rothlisberger, D., Pos, K. M. & Pluckthun, A. (2004). *FEBS Lett.* **564**, 340–348.
Schafmeister, C. E., Miercke, L. J. & Stroud, R. M. (1993). *Science*, **262**, 734–738.
Shea, C., Bloedorn, L. & Sullivan, M. A. (2005). *J. Struct. Funct. Genomics*, **6**, 171–175.
Slovic, A. M., Kono, H., Lear, J. D., Saven, J. G. & DeGrado, W. F. (2004). *Proc. Natl Acad. Sci. USA*, **101**, 1828–1833.
Slovic, A. M., Summa, C. M., Lear, J. D. & DeGrado, W. F. (2003). *Protein Sci.* **12**, 337–348.
Stura, E. A., Taussig, M. J., Sutton, B. J., Duquerroy, S., Bressanelli, S., Minson, A. C. & Rey, F. A. (2002). *Acta Cryst.* D**58**, 1715–1721.
Vagin, A. & Teplyakov, A. (1997). *J. Appl. Cryst.* **30**, 1022–1025.
Zhou, Y., Morais-Cabral, J. H., Kaufman, A. & MacKinnon, R. (2001). *Nature (London)*, **414**, 43–48.